Calculated and measured Auger line shapes in SiO_2

D. E. Ramaker, J. S. Murday, and N. H. Turner
Naval Research Laboratory, Washington, D.C. 20375

G. Moore and M. G. Lagally
University of Wisconsin, Madison, Wisconsin 53706

J. Houston
Sandia Laboratory, Albuquerque, New Mexico 87115

(Received 2 October 1978)

The Si $L_1L_{23}V$, Si $L_{23}VV$, and O KVV Auger transitions in SiO_2 have been measured and compared to calculated line shapes. The measurements were made on thick steam oxides grown on Si (111). The data were corrected for electron loss and spectrometer distortions; the correction scheme is presented. All three Auger transitions are calculated from the same valence-electron density of states which is described in terms of a linear-combination-of-atomic-orbitals molecular-orbital model. X-ray photoelectron spectroscopy and x-ray emission and absorption data are used to determine the orbital energies, populations, and widths. The Auger transition energies are estimated from one-electron calculations including static relaxation and hole-hole repulsion effects. The intensities are estimated from electron densities local to the core hole multiplied by the appropriate atomic Auger matrix element. Three major features are predicted by the calculations for the Si $L_{23}VV$ and O KVV transitions and are observed experimentally; two major features are predicted for Si $L_1L_{23}V$, only one is observed experimentally because of baseline problems. The calculated absolute energies of all major features agree within 2 eV with experimental values, the relative agreement between peaks within a given line shape is better than 1 eV. The observed intensities of the major features are in reasonable agreement with the calculations but there are some discrepancies thought due to either the matrix elements or the charge densities assumed in the calculations. Considerable intensity in the experimental line shapes between the major peaks, not accounted for in the present calculation, is probably due to shake-up or shake-off satellite structure.

I. INTRODUCTION

The interest in the electronic structure of SiO_2 has resulted in numerous theoretical and experimental investigations of the valence-electron density of states. The theoretical approaches include empirical and semiempirical molecular-orbital (MO) calculations on clusters of Si_2O,[1] SiO_4,[2] and larger aggregates,[3] nonempirical calculations also involving Si_2O,[4,5] SiO_4,[5-8] and larger clusters,[5] *ad hoc* band-theoretical approaches,[9,10] and a self-consistent pseudopotential calculation.[11] The experimental measurements of the valence-electron density of states have included photoemission[12-15] and x-ray emission.[16-19] A reasonably consistent model of the valence-electron states has been distilled from this work[9,11,15] and is in close correspondence to a similar model for the silicates as distilled from the corresponding spectra.[20] The present state of agreement between the various theories and experimental data has been discussed in several recent papers.[9,11] In essence, there are three major groups of valence electrons commonly referred to as the "O_{2s}" bonding states about 20 eV below the valence-band edge, the "O_{2p}" bonding states grouped about 6 eV below the edge, and the O_{2p} nonbonding states located just below the edge. The O_{2p} nonbonding states are almost entirely localized on the oxygen atoms while the bonding states have substantial amounts of electron density residing on the silicon atoms.

While the photoemission (PES) measurements are surface sensitive, they sample the entire electron density and do not provide ready identification of local electron densities. The x-ray emission (XES) and absorption measurements, on the other hand, do provide direct information on the local electron density of states but are not surface sensitive. Auger electron spectra (AES), while difficult to interpret, can provide a surface-sensitive measure of the local density of states. The local valence-electron structure can be used to define the chemical state of an atom. If this information can be extracted from AES, then its much smaller spatial resolution might be used to determine bonding in areas much smaller than now possible with x-ray photoelectron spectroscopy (XPS). The "chemical shift" of the Si LVV Auger line has been utilized for just this purpose.[21]

The chemical information in AES is, however, not limited to the transition energy, which is often difficult to measure on an absolute scale.

Far more information is available from the Auger line shape. Within the past few years, there has been increasing evidence that Auger line shapes may be useful in interpreting the chemical environment of atoms on solid surfaces.[22-28] The first quantitative interpretation of an Auger line shape observed from a solid, in which the Auger matrix effects were included, was for the Si $L_{23}VV$ line from a Si (111) surface.[29] It revealed a strong emphasis on the p-like valence states, a deemphasis of the s-like states, indicating a strong Auger-matrix-element dependence. More recent quantitative efforts have been limited to the elemental solids, [e.g., Si, Li, Be, Cu, Zn, Ge, and Ga (Refs. 30–35)] where similar effects are observed.

In the gas phase the description of molecules by the MO theory is basic. Good agreement between experimental and theoretical Auger line shapes have been obtained for several molecules [these include H_2O, NH_3, CH_4, C_2H_2, C_2H_4, and CH_3OH[36-39]] using a fold of one electron MO's as a description of the two-hole final density of states (DOS). Hole-hole correlation effects (configuration mixing) are expected to be small because the effective hole-hole interaction U is small relative to the nearest-neighbor bonding interactions V. In highly ionic solids the final two-hole DOS is expected to be adequately obtained from an MO on the appropriate ion (e.g., to describe the Li_2SO_4 S Auger line shape, the MO description of the SO_4^{2-} anion would be appropriate[40]). Finally in most s and p band metals (e.g., Al, Si, Li, Ag[27,28,41,42]) the Auger line shape reflects a DOS similar to that generated from a fold of the one-electron valence bands. However, in certain narrow-d-band conductors [e.g., Cu, Zn, Ni (Refs. 33–35)], the CVV line shape reflects an atomiclike final state; i.e., the Auger decay proceeds as if it involved isolated atoms. This has been attributed to hole-hole correlation effects (configuration mixing) which now are large because the hole-hole interaction energy U is large relative to the band width Γ.[43,44] If $U > 2\Gamma$, energy conservation forces the two holes to remain on the atom in which they were created yielding an atomiclike spectrum.[35,43,44]

The extension to SiO_2 is indeed an interesting one. The rather large covalent-bonding interaction between Si and O suggests a large nearest-neighbor interaction V, but a smaller interaction of the Si or O atom with the remaining solid ($\Gamma < V$). If the effective hole-hole interaction U is large relative to both V and Γ, one expects the Auger line shape to reflect the atomic DOS as in the case of the d-band metal and the effective hole-hole interaction is just the one-center atomic repulsion energy. If, on the other hand, U is intermediate between V and Γ(i.e., $V > U > \Gamma$) one might expect a one-electron MO model on some appropriate cluster (e.g., SiO_4^{4-} or Si_2O^{6+}) to adequately describe the final two-hole DOS. This is true because strong mixing will occur within each band distorting and narrowing the two-hole DOS one would get from a simple fold of the one-electron valence band; but little mixing will occur between the bands. Furthermore, the effective U is now expected to be the interaction of two holes localized on the central atom and its nearest neighbors; i.e., the molecular cluster. In the event that $U < \Gamma < V$, we would expect a simple fold of the one-electron band DOS to be revealed, and the holes become completely delocalized ($U \to 0$).

In this work we will describe the final two-hole DOS by a fold of the one-electron MO's on the clusters SiO_4^{4-} and Si_2O^{6+}. It is recognized that our results will be cluster-size dependent, however, it is also well known that with increasing cluster size the one-electron MO DOS asymptotically approaches the band DOS. We began this section with a review of the literature which demonstrated that the band DOS can be adequately described in terms of the SO_4^{4-} and Si_2O^{6+} clusters. Furthermore, the effective hole-hole interaction U asymptotically goes to zero with increasing cluster size as it is in the band model. In the event that $U > V > \Gamma$, the effective hole-hole interaction should approach the one-center atomic interaction potential on the central atom (the atom with the original core hole). The cluster MO approximation will reasonably approximate this provided the "central" atom appears only once in the cluster. Thus the cluster should include only the central atom and its nearest neighbors to cover the range of possibilities. We will reconsider some of these assumptions in the discussion, Sec. IV. In this work we will examine the Si $L_1L_{23}V$, Si $L_{23}VV$, and O KVV Auger line shapes. Since all three Auger lines involve the same valence bands, the simultaneous calculation of the three line shapes provides a good test of the theoretical approach.

II. EXPERIMENTAL

Measurements were made on ~1500-Å-thick steam oxides grown on 3-Ω cm Si(111).[45] Operating pressures without bakeout were in the low 10^{-10} Torr range. The surfaces were sputter etched with a Xe-ion beam at 500 eV and 30 mA until the surface contamination, consisting mostly of carbon, was below detectability limits. The data were taken with a PEI single-pass cylindrical

mirror analyzer with coaxial electron gun, with an incident-beam voltage of 1 kV and a beam current of 10 μA. In order to avoid decomposition of the SiO_2 by the electron beam, an oxygen partial pressure of $\sim 1 \times 10^{-7}$ Torr was maintained during the measurements. A check on the contamination level after measurement indicated that the surface remained clean. Energy-loss spectra agreed with those reported in the literature.[46] First-derivative $[dN(E)/dE]$ spectra were taken at a 1-eV peak-to-peak modulation. These were signal averaged for time periods, usually less than $\frac{1}{2}$ h, depending on the strength of the Auger line.

Data reduction consisted of subtracting an appropriate background, integrating the spectra to give $N(E)$, deconvoluting with a function that approximates the instrument response and the energy losses suffered by an outgoing Auger electron, and scaling by a function representing the change in transmission of the analyzer and gain of the detector over the energy range of the Auger line. The merits of this approach and an alternative data reduction methodology are discussed in Ref. 47.

In the case of the dN/dE spectra at energies below 200 eV, where the secondary electrons dominate, the background can be fitted either by a simple polynomial or a function of the form[48]

$$B\frac{dN}{dE} \sim \frac{1}{(E-E_0)^{1.3}}, \tag{1}$$

where B is a constant and E_0 is adjusted to one point on the dN/dE curve. This background subtraction was used here, with $E_0 = 12$ eV. The shape of the $L_{23}VV$ line, because it is at higher energies where the background is slowly varying, is quite insensitive to reasonable ranges for the choice of background. The $L_1L_{23}V$ line, which lies in a region of rapidly varying background, is much more sensitive to the background subtraction. After the background is removed, the lines are integrated. An example of the integral spectrum, $N(E)$, for the Si $L_{23}VV$ line is shown in Fig. 1. Part of the $L_1L_{23}V$ line is also visible.

As the Auger electrons propagate through the lattice, they experience energy losses, which redistribute the electrons along the energy scale. The electron energy analyzer and detector also contribute distortions to the Auger line shape. The loss function and instrument response for each Auger transition can be approximated by the backscattered spectrum of an electron beam with primary energy equal to the energy of the respective Auger transition[42,49]; while this is an approximation, it appears to give quite good results.[20,27,28,41,42,50,51] An example of the loss spectrum is shown as the bottom curve in Fig. 2. Using the Van Cittert method,[52] the function is deconvoluted from the $N(E)$ spectrum, resulting in an Auger spectrum such as shown in Fig. 2.

The use of an instrument loss function measured at only the main peak of the Auger line makes two assumptions, that there are no diffraction effects and that the function does not change with energy. For the amorphous film

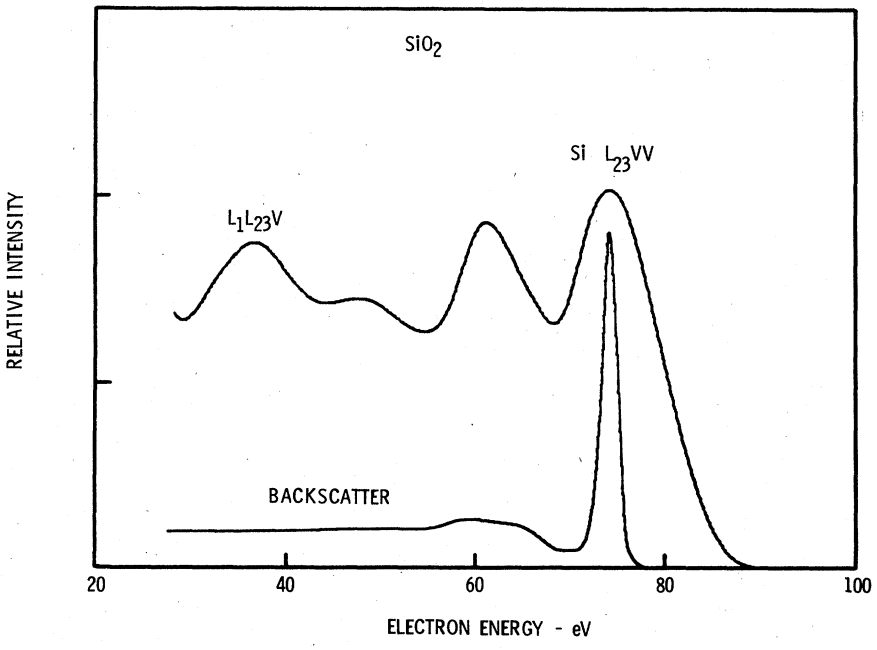

FIG. 1. $N(E)$ Auger spectrum of the Si $L_{23}VV$ transition and corresponding backscatter spectrum at the energy of the main feature.

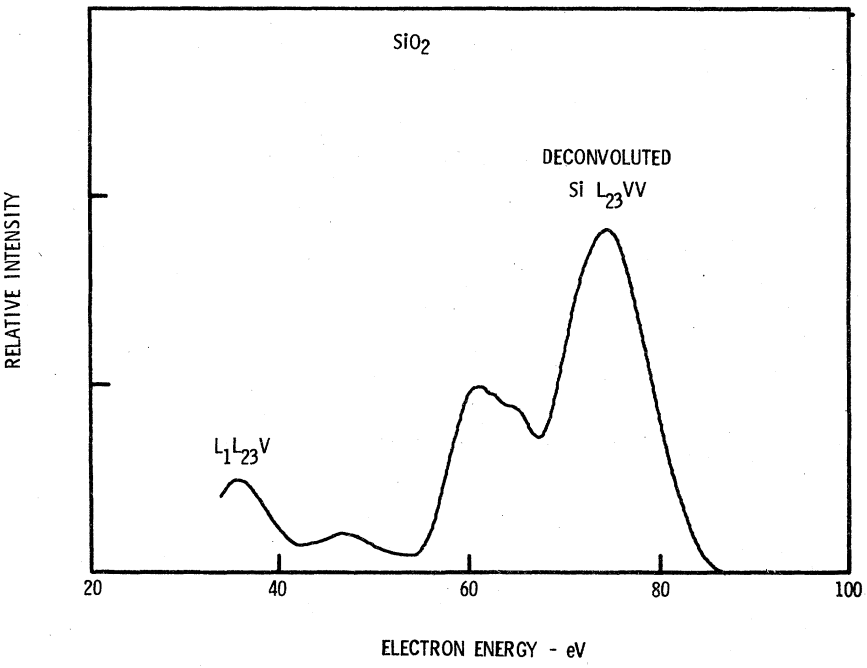

FIG. 2. Auger spectrum of the Si $L_{23}VV$ transition and part of the Si $L_1L_{23}V$ transition after deconvolution.

considered here, diffraction effects are not a problem. The $N(E)$ spectra are slightly distorted due to energy dependence in the instrument response. We have approximated the effect here by scaling the deconvoluted Auger line by a transmission factor estimated for the analyzer. The electron loss in the sample also has an energy dependence which is characterized by the energy dependence of the inelastic mean free path. For the Si $L_{23}VV$ and O KVV lines, the energy variation is small and no corrections are made. For the Si $L_1L_{23}V$ line, the knowledge of the mean free path is poor and the Auger line width is narrow ($\sim<20$ eV), so again no correction is made.

The resulting Auger line shapes for the Si $L_1L_{23}V$, Si $L_{23}VV$, and O KVV lines are shown, respectively, as the solid lines in Figs. 4(a), 5(a), and 6(a).

III. CALCULATION OF THE AUGER TRANSITIONS

A. Theoretical formulations

The Auger transitions are calculated by assuming the valence electron DOS in SiO_2 can be described in terms of the cluster linear-combination-of-atomic-orbitals–molecular orbital (LCAO–MO) model as discussed above. The transitions will involve the appropriate core hole, Si L_1, L_{23}, or O K, coupling with the local electron DOS as represented by the occupation of the atomic orbitals centered on that atom (i.e., atom with the core hole). In the next few paragraphs we will present the expressions from which we calculate the transition energies, intensities and line widths.

The transition energies will be calculated from the formulation of Shirley and co-workers[26]

$$E_{KXY}(Z) = E^0_{KXY} + R(X, Y) - F(X, Y), \tag{2}$$

where E^0_{KXY} is the transition energy deduced from the one-electron binding energies referenced to the Fermi level, R is an intraorbital and outer-atomic-orbital relaxation term, and $F(X, Y)$ is a two-electron interaction energy describing the coupling of the final-state holes. Our adaptation of this formula from atoms to molecules, in particular the $R(X, Y)$ and $F(X, Y)$ terms, will be described in more detail elsewhere.[40]

The transition intensities are calculated from the expression

$$I_{KXY} \propto \sum_{n,m} c^2_{Xn} c^2_{Ym} P_{Knm}, \tag{3}$$

where c^2_{Xn} and c^2_{Ym} are the populations of the n, m atomic orbitals on the central atom in the X, Y molecular orbitals, respectively, and P_{Knm} is the appropriate atomic Auger matrix element obtained from the results of McGuire[53] and Walters and Bhalla.[54] Two-center terms are ignored, which means that the sum in Eq. (3) reduces to a single term for all cases considered here.

Each transition will be represented by a Gaussian function centered about the transition energy and whose area is proportional to the cal-

culated intensity. The line widths of the Gaussians are calculated from

$$\Gamma_{KXY} = \Gamma_K + \Delta_X + \Delta_Y + 2K, \quad (4)$$

where Γ_K is the core level width, $\Delta_{X,Y}$ are the valence level widths, and $2K$ is the singlet-triplet splitting. The latter is added in when it is of the order of or less than the other line width contributions. Otherwise the singlet and triplet final states are considered separate transitions. A simple summation of the contributions is used because the various sources of line width are not all Gaussian or Lorentzian or any other common functional form, i.e., the Γ_K and $2K$ contribution may account for nonresolved lines.

B. Empirically derived parameters

1. Energy

The valence-electron energy levels for SiO_2 have been probed by photoemission,[12-15] and by Si K_β[18,19] and O K_α[16,17] x-ray emission spectra. Fisher *et al.*[15] have correlated these measurements so that they can be compared to each other on the same absolute energy scale (see Fig. 3). As discussed by several workers,[9,11,15] the six orbitals can be grouped into three pairs (see Table I; we will use the T_d notation to identify the orbitals): $4a_1$ and $3t_2$ represent predominantly O_{2s} electrons bonding with admixtures of Si_{3s} and Si_{3p}, respectively; $5a_1$ and $4t_2$ represent bonding orbitals with O_{2p} added to Si_{3s} and Si_{3p}, respectively; $(5t_2, 1e)$ and $1t_1$ represent the predominantly nonbonding O_{2p} orbitals. The energy of the peaks is given by Fischer *et al.*[15] relative to the edge of the valence band. If we assume the Si $2p$ binding energy relative to the Fermi level to be 103 eV,[20,55,56] we are led to a value of ~5 eV between the top of the valence band and the Fermi level. The O 1s binding energy is thereby required to be 533 eV (relative to Fermi level) which is in agreement with literature values.[55,56] The one-electron binding energies of the various electron levels to be used in this paper are summarized in Table I.

When calculating the oxygen Auger line shape we use the C_{2v} symmetry. The O_{2p} nonbonding electrons occupy the $2b_1$ and $7a_1$ orbitals in this symmetry class. The $2b_1$ orbital is perpendicular to the plane of the Si-O-Si cluster and is completely nonbonding. The $7a_1$ orbital lies in the plane and thereby does have some bonding aspect; Pantelides[9] identifies the $7a_1$ contribution with the shoulder at 4 eV in the O K_α spectrum (Fig. 3). Since they are close in energy compared to the Auger line widths, we have chosen to identify both the $2b_1$ and $7a_1$ orbitals with a common energy

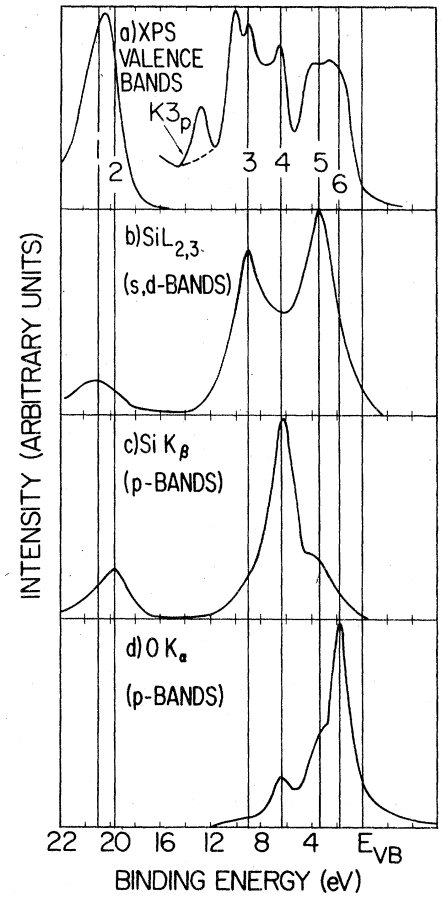

FIG. 3. Composite of the XPS, Si L_{23}, Si K_β and O K_α x-ray emission spectra produced by Fischer *et al.* (Ref. 15) for SiO_2.

as shown in Table I. Pantelides[9] also points out that the data in Fig. 3 shows evidence for banding effects in the "O_{2p}" bonding group. The oxygen electron density, as measured by the O K_α x-ray emission, is concentrated at an energy appropriate to the $4t_2$ orbital, i.e., at the top of this bonding group. The concentration of O_{2p} at the $4t_2$ energy may reflect the tendency for p electrons to dominate at the top of a band. Similarly the XPS peak in the "O_{2s}" bonding group, which predominately samples the O_{2s} electrons, is slightly displaced toward the $4a_1$ orbital. This may reflect the tendency of s-like electrons to dominate the bottom of a band. As is evident from Table I, we have chosen the $5b_2$ and $6a_1$ orbital energies to reflect these observations.

The two-electron interaction energy $F(X, Y)$ and the relaxation energy $R(X, Y)$ need to be defined within the MO model. Assuming the Slater integral F^0 is the dominant term and utilizing the zero differential overlap approximation in $F(X, Y)$,

TABLE I. One-electron binding energies and valence orbital linewidths in SiO_2.

Orbital group	C_{2V} (Si_2O) designation	Δ (eV) [c]	T_d (SiO_4) designation	Δ (eV) [c]	Energy [a] (eV)
O_{2p} nonbonding	$2b_1$, $7a_1$	3.3	$1t_1$, $1e$, $5t_2$	1	8 (5,6) [b]
"O_{2p}" bonding	$5b_2$	1.5	$4t_2$	1.5	11 (4)
			$5a_1$	1	14 (3)
"O_{2s}" bonding			$3t_2$	2	25 (2)
	$6a_1$	2	$4a_1$	2	27 (1)
Si_{2p}					103
Si_{2s}					154
O_{1s}					533

[a] Energies referenced to Fermi level.
[b] Refers to the peak designations in Fig. 3.
[c] Estimated from XES and XPS data.

TABLE II. Calculated Auger transitions [from Table I(b) populations].

Silicon			E^0_{KXY} [b]	$R(X,Y)$	$F(X,Y)$ [a]	E_{KXY} [a] (eV)	I [c]	K	Γ (eV)
L_1 L_{23}	V	V							
	$4a_1$	$4a_1$	24	9.4	−7.2	25	0.5	···	5.2
	$3t_2$		26	9.4	7.0	28	0.3		5.2
	$5a_1$		37	8.6	−7.3	38	1.7	···	4.2
	$4t_2$		40	8.4	−6.6	41	1.8	···	4.7
L_{23} V	V								
$4a_1$	$3t_2$		51	5.5	−8.0	49	0.1	3.3	11.8
$3t_2$	$3t_2$		53	5.5	−8.2	50	0.2	3.6	12.4
$3t_2$	$5a_1$		64	4.8	−6.9	62	0.4	···	4.3
$4a_1$	$4t_2$		65	4.4	−6.7	62	0.8	···	4.7
$3t_2$	$4t_2$		67	4.5	−6.9	64	2.8	0.1	4.9
$5a_1$	$4t_2$		78	3.8	−5.7	76	2.4	1.0	5.7
$4t_2$	$4t_2$		81	3.5	−5.6	79	7.6	1.4	6.9
$4t_2$	$5t_2$		84	4.7	−7.0	82	0.3	4.7	13.1
Oxygen									
K V	V								
$6a_1$	$6a_1$		479	5.5	−18.4	466	1.0	···	4.2
$6a_1$	$7a_1, 2b_1(S)$		498	5.7	−19.3	481	2.0	3.8	5.5
$6a_1$	$5b_2(S)$		495	4.6	−12.5	485	0.5	1.9	4.4
$6a_1$	$7a_1, 2b_1(T)$		498	5.7	−19.3	488	0.5	3.8	5.5
$6a_1$	$5b_2(T)$		495	4.6	−12.5	489	0.1	1.9	4.4
$7a_1$	$7a_1$		517	6	−21.9	501	3.1	···	6.8
$2b_1$	$2b_1$								
$7a_1$	$2b_1(S)$		517	6	−19.7	502	2.0	1.1	6.8
$5b_2$	$5b_2$		511	3.6	−9.9	505	0.4	···	3.2
$5b_2$	$7a_1, 2b_1(S)$		514	4.8	−12.6	506	2.0	0.5	5.0

[a] $F(X,Y)$ is calculated only from $F^0(n,m)$ terms for Si, from F^0 and F^2 terms for O.
[b] Energies measured relative to Fermi level. E_{KXY} includes a term $\pm K$ for those transitions designated singlet (S) or triplet (T), respectively.
[c] The intensities are related only for the common core hole; no attempt is made here to relate the Si $L_1L_{23}V$, $L_{23}VV$, and O KVV total intensities. When (S) or (T) is absent the total intensity, singlet plus triplet, is given for the transition if both exist.

$$F(X, Y) = \sum_{nm} c^2_{Xn} c^2_{Ym} F^0(n, m),$$

where c^2_{Xn}, c^2_{Ym} are the atomic-orbital populations projected out of the X, Y molecular orbitals, respectively. The sum includes all atomic-orbital contributions to the molecular orbital, i.e., orbitals on the central atom as well as the ligand species, and includes both one-center and two-center terms. For Si as the central atom, the higher-order Coulomb and exchange integrals are neglected in the determination of the transition energy (in part they will be used to calculate linewidth contributions). For oxygen as the central atom, the higher-order one-center Slater integrals are included. All Slater integrals are obtained from the tabulation of Mann.[57]

The relaxation energy in the atomic calculations can be broken into four components: inner, intra, and outer shell on the central atom, and extra atomic. We have ignored the inner-shell relaxations as negligible in analogy to the atomic case. The intrashell relaxation is an appropriate average, $R_x = \sum c^2_{Xn} r_n$, of the atomic intraorbital relaxation terms r_n. For the oxygen $2s$ and $2p$ orbitals we take the 6 eV calculated by Shirley[58] for atomic Ne; this probably overestimates the intrarelaxation energy on oxygen. For the silicon $3s$ and $3p$ we take the values of 2 and 1 eV, respectively, calculated by Gianturco and Coulson[59] for the $3s$ and $3p$ orbitals on sulfur. Following Shirley we define the relaxation involving two molecular orbitals $R(X, Y) = \frac{1}{2}(R_X + R_Y)$. The O KVV and Si LVV transitions both leave their hole states in the outermost electron levels so the outer-shell relaxation does not exist. We have ignored the extra-atomic relaxation. For the Si $L_1L_{23}V$ transitions the outer-shell relaxation is calculated using the equivalent-cores approximation of Shirley[58] for the Si_{2p} orbital.

Table II presents the Auger transition energies as well as the values of E^0, $F(X, Y)$, and $R(X, Y)$ for the experimental choice of local electron densities. The choice of these densities is the subject of Sec. III B 2.

2. *Intensities*

We have calculated the Auger transitions for three different choices of local electron populations: (a) c_n determined from the work of Tossell on a SiO_4^{4-} cluster, (b) c_n determined from the work of Yip and Fowler on a Si_2O^{6+} cluster, and (c) c_n determined largely from the x-ray emission intensities and electron state counting.

The nonempirical MO calculations of Tossell[7] on SiO_4^{4-} provide a set of atomic-orbital populations to use in the calculation of the Auger line shape. The atomic-orbital populations as described by Tossell are presented in Table III(a). Note that the net charge state is $Si^{+2.22}$ and $O^{-1.58}$ due to the representation of an orthosilicate ion SiO_4^{4-}. While SiO_2 might be written as $Si^{4+}(SiO_4)^{4-}$, by symmetry there can in fact be no difference in the charge states of the two Si atoms. One would expect, therefore, that in SiO_2 some of the charge which Tossell indicates resides on the O in $(SiO_4)^{4-}$ will flow back to the silicon atom.

The LCAO–MO calculations of Yip and Fowler[5] on Si_2O^{6+} also provide a set of atomic-orbital populations to use for the Auger calculations. The atomic-orbital populations as derived from Yip and Fowler are presented in Table III(c). The net charge states are $Si^{+3.57}$ and $O^{-1.14}$.

The x-ray emission data suggest a way to adjust the populations of the SiO_4^{4-} cluster to more ac-

TABLE III. Filled valence orbital compositions. Number of electrons per atom.

		SiO_4^{4-} [a]				$(SiO_2)_2$ [b]				Si_2O^{6+} [c]				
		Si		O		Si		O		Si		O		
Orbital group	T_d	$3s$	$3p$	$2s$	$2p$	$3s$	$3p$	$2s$	$2p$	$3s$	$3p$	$2s$	$2p$	C_{2V}
	$1t_1$	···	···	···	1.50	···	···	···	1.50	···	···	···	2.00	$2b_1$
O_{2p} nonbonding	$1e$	···	···	···	1.00	···	···	···	1.00	···	···	···	2.00	$7a_1$
	$5t_2$	···	0.06	···	1.48	···	···	···	1.50					
"O_{2p}" bonding	$4t_2$	···	1.14	···	1.21	···	1.50	···	0.75	0.15	0.21	···	1.28	$5b_2$
	$5a_1$	0.34	···	0.05	0.41	0.50	···	···	0.25					
"O_{2s}" bonding	$3t_2$	···	0.18	1.45	···	···	0.27	1.36	···					
	$4a_1$	0.06	···	0.48	···	0.15	···	0.43	···	0.03	0.04	1.86	···	$6a_1$
Mulliken charge		0.40	1.38	1.98	5.60	0.65	1.77	1.79	5.00	0.18	0.25	1.86	5.28	

[a] Reference 7.
[b] Deduced from experimental data as outlined in text.
[c] Reference 5.

curately represent SiO_2. First note that the four electrons on the silicate can be attributed to neighboring silicons in silicon dioxide, so the T_d cluster orbitals represent the filled orbitals of $(SiO_2)_2$. The O_{2p} nonbonding orbitals were shown in both the Si_2O^{6+} and SiO_4^{4-} clusters to be essentially pure O_{2p}. Given the eight orbitals in the combined $1t_1$, $1e$, $5t_2$ nonbonding group, there are 16 nonbonding electrons localized on the four oxygens. The O K_α x-ray emission spectrum has an intensity ratio of about 4:1 between the nonbonding and bonding O_{2p} orbitals. This requires four electrons to be localized on the four oxygens in the "O_{2p}" bonding group. The "O_{2p}" bonding group has four filled orbitals or eight electrons. The remaining four electrons must be localized on the Si in the Si $3p$ and Si $3s$ orbitals. The O_{2p} bonding orbitals in T_d symmetry split into a triply degenerate t_2 and an a_1 component. If we divide the four Si electrons equally among the four orbitals, then there will be three Si $3p$ and one Si $3s$ electrons in the O_{2p} bonding group. This choice of distribution is somewhat arbitrary and must be checked by the comparison of the calculated Auger line shapes to those measured.

The Si K_β shows a low-energy peak with (15–20)% of the main peak intensity and the Si L_{23} shows a similar peak with (20–25)% of the main peak intensity. (We have chosen for the moment to ignore the anomalously large highest energy peak in the Si L_{23}; no satisfactory explanation for this peak has been found. We will come back to this point in the discussion.) Therefore, the "O_{2s}" bonding group must have ~0.54 and 0.30 Si $3p$ and $3s$ electrons, respectively. The $3s$ contribution is a bit larger than the intensity ratio itself since the L_{23} cross section contains the factor $(\Delta E)^3$ which is significant for the Si L_{23} transitions. This leaves room for 7.2 O_{2s} electrons in this group, which fill the remaining states in the $3t_2$ and $4a_1$ orbitals. A summary of the charge distribution outlined above is presented in Table III(b). The valence charge state is $Si^{+1.6}$ and $O^{-0.8}$.

Note that compared with the Tossell charge state, the $(SiO_2)_2$ orbital populations do show the expected increase of Si electrons. The $(SiO_2)_2$ charge state is essentially determined by the 4:1 ratio of intensities assumed for the two peaks in the O K_α spectra. Gilbert *et al.*[4] estimate that 4:1 is a lower limit and 8:1 is an upper limit. If we were to choose a larger ratio, the effect would be to lower the number of electrons on O and increase them on Si. This would bring the Si net charge state even closer to the charge state of Si^{+1}, that estimated by Gilbert to be the most reasonable. However, since we have no firm rationale for doing so, we will stay with the populations inferred above.

The Auger transition intensities for the $(SiO_2)_2$-derived populations are presented in Table II. The intensities are calculated from Eq. (3) where the values of c are obtained by converting the electron charge in Table III to a fraction of orbital occupation. For instance, the Si $3p$ occupation of the $4t_2$ orbital is 1.5 electrons times 2 Si atoms divided by 6 available t_2 states giving c to be 0.5.

3. *Line widths*

Three contributions to the line widths are estimated for each transition: (a) The core level width, (b) the valence orbital width, and (c) contributions due to the singlet-triplet splitting in the final-state hole-hole interaction. The core level widths are taken to be $\Gamma(O_{1s}) = 0.2$ eV and $\Gamma(Si_{2s}) = 2$ eV estimated from lifetime broadening[53]; $\Gamma(Si_{2p}) = 1.2$ eV estimated from the spin-orbit splitting.[60] The valence orbital widths can be estimated from the x-ray emission and photoemission data and are presented in Table I.

The singlet-triplet energy differences $2K$ for the various two-hole final states were calculated from one-center Slater integrals. Where this energy was of the order of the line width contributions above, the $2K$ values were added into the line width. In the O KVV transitions, the magnitude of $2K$ was large enough to require separate transitions for the singlet and triplet final states. (Large-K values occur for Si also, but only for small intensity transitions.)

The Auger line widths calculated for the $(SiO_2)_2$-derived populations are presented in Table II.

IV. RESULTS AND DISCUSSION

When comparing the calculated and experimental line shapes, two parameters have been allowed to vary. The first is a multiplicative constant which simply adjusts the total intensity of the calculated line shape. This parameter is necessary because there has been no attempt at absolute quantification. The second parameter, δE, permits the full calculated line shape to be shifted up or down in energy. The δE could reflect sample charging shifts, extra-cluster relaxation energies, or other processes which would not change the line shape, but would affect the Auger kinetic energies. These two parameters were determined by forcing the pinnacle of the major peak in the Si $L_{23}VV$ and O KVV to align with its experimental counterpart. The Si $L_1L_{23}V$ was aligned by requiring the energy of the high-energy shoulder to agree with the experiment and then determining the intensity factor by least-squares

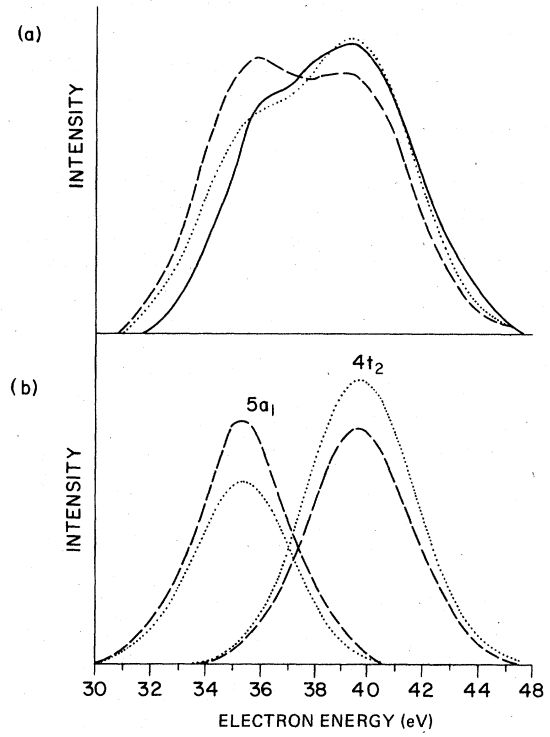

FIG. 4. (a) Comparison of the experimental (solid line) Si $L_1L_{23}V$ Auger transitions with those calculated from the $(SiO_2)_2$ populations (dashed line) and from the modified $4t_2$, $5a_1$ populations (dotted line). (b) $4t_2$ (40 eV) and $5a_1$ (35 eV) contributions to the $L_1L_{23}V$ line shape.

fit to the top of the entire peak.

The comparison of calculated and experimental line shapes for the Si $L_1L_{23}V$ transition is most straightforward because it does not involve the self-convolution of the valence density of states. The comparison of the measured $L_1L_{23}V$ line shape and the line shape calculated from the $(SiO_2)_2$-derived orbital population [Table III(b)] is shown in Fig. 4. This feature is only that part of the full line shape which originates from the "O_{2p}" bonding group. As can be seen in Table II, there should be an additional feature about 10 eV lower in kinetic energy with about one-sixth the intensity which corresponds to the "O_{2s}" group. There is, in fact, structure observed in $d^2N(E)/dE^2$ spectra in the appropriate energy region but it could not be separated cleanly from secondary electron contributions in the base line.

There are two transitions which contribute to the $L_1L_{23}V$ line shape presented as the dashed line in Fig. 4; the higher-energy peak corresponds to the $4t_2$ orbital, the lower-energy peak to the $5a_1$ orbital. The measured $5a_1$ orbital contribution would actually be slightly reduced [(5–20)%] in magnitude if one corrected the data for the electron sampling depth since the mean free path in this energy region is beginning to increase sharply as energy decreases. If the assumed matrix elements are correct, then the discrepancy between the calculated (dashed line) and measured intensities shown in Fig. 4 is a reflection of the relative populations of the Si 3*s* and 3*p* in the $5a_1$ and $4t_2$ orbitals, respectively. Recall that the relative Si 3*s* and 3*p* populations of these two molecular orbitals were established in a somewhat arbitrary fashion. If one wished to turn the process around, the Auger line shape provides a mechanism to test those relative populations. The dotted line in Fig. 4 shows just such a fit where the Si 3*p* contribution to the $4t_2$ orbital in Table III(b) was increased by only 10% and the Si 3*s* contribution to the $5a_1$ orbital was decreased by 30% so as to keep the same net charge. Since no charge need be transferred between the orbital groups, such an adjustment would not affect the major features in the Si $L_{23}VV$ and O KVV line shapes. The small corrections indicated by the fitted populations suggests that the initial assignments are reasonable; the corrections cannot be considered quantitative until we have more accurate matrix elements and have corrected for any line-shape distortions.

The theoretical energies had to be shifted down by less than 2 eV to bring about the registry of the calculated and measured $L_1L_{23}V$ transitions. This is well within the uncertainties of the measured Auger energy, of the XPS binding energies, and of our calculations. The line width is slightly overestimated (by ~1 eV out of 7 eV) but the agreement is also considered to be acceptable given the approximations made.

The Si $L_{23}VV$ calculated line shape from the $(SiO_2)_2$ populations and the measured line shapes are compared in Fig. 5. The theoretical energies had to be shifted down by less than 1 eV. There was no significant change in the calculated line shape with the Tossell populations. The calculated $L_{23}VV$ line shape is dominated by the ratio of the Si populations in the $3t_2$ and $4t_2$ orbitals; the $(SiO_2)_2$ and Tossell populations do not differ much in that regard.

The intensities of the calculated peaks at 64 and 50 eV are too weak. One can postulate several explanations for this discrepancy. The assumed matrix elements and/or electron populations may be wrong. We have tried to simply rearrange the populations to achieve better agreement, but were not successful in finding new populations which were consistent with the x-ray emission data. It may be that the AES and XES sample different electron populations. A second possibility is that the base-line and electron-loss corrections to

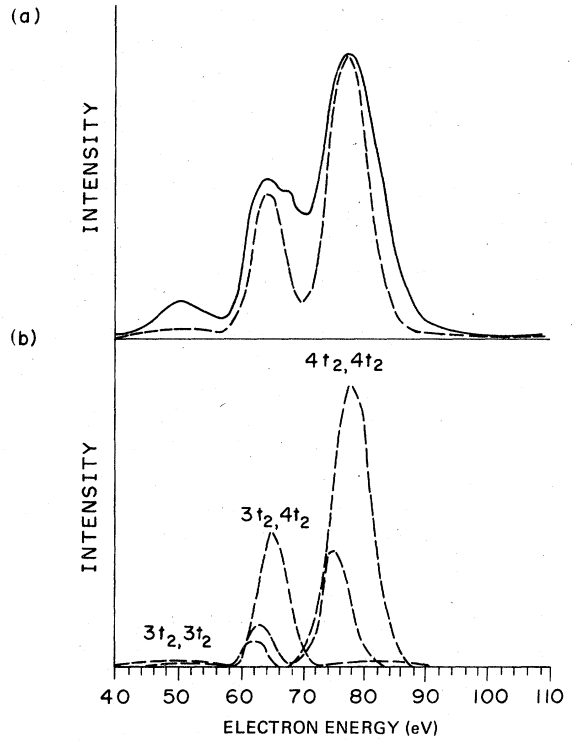

FIG. 5. (a) Comparison of the experimental (solid line) Si $L_{23}VV$ Auger line shape with those calculated from the $(SiO_2)_2$ populations (dashed line). The peak at 78 eV involves transitions with both valence electrons from the O_{2p} bonding group; the peak at 64 eV, one each from the O_{2p} and O_{2s} groups; the peak at 50 eV, both from the O_{2s} group. (b) The major Auger transitions arising from the individual molecular orbitals which have local Si electron density. The origin of each peak may be identified from Table II.

the data were inadequate and left too much apparent intensity in the 50-eV peak. A third possibility, namely, unaccounted contributions from the $L_1L_{23}V$ transition, will be discussed later. A second discrepancy between the calculated and observed line shape lies in our underestimation of the intensities between the major peaks. This is in large part due to our ignoring the contributions resulting from shake-up and shake-off. These processes account for ~(20–40)% of the total intensities in Ne and Ar gas-phase Auger spectra[61,62] and may account for much of this discrepancy.

Since the Si $L_1L_{23}V$ and $L_{23}VV$ data in Fig. 2 was taken under the same conditions and the loss correction involved the same measured loss peak, it is possible to compare the relative measured areas of these two transitions with the theoretical rates for electron excited Auger transitions. For a 1-keV electron beam the ratio of the theoretical cross sections for Si L_1 and $L_{2,3}$ core ionization is $\sigma_{L_{23}}/\sigma_{L_1} = 7.3$.[63] The ionized cores will most probably deexcite via $L_1L_{23}V$ and $L_{23}VV$ processes. If every L_1 core hole results in both a $L_1L_{23}V$ and $L_{23}VV$ process, then the observed ratio should be 8.3; if no $L_1L_{23}V$ event is followed by an $L_{23}VV$ event then the ratio would be 7.3. The observed ratio can be estimated from Fig. 2, if one multiplies the $L_1L_{23}V$ area in Fig. 2 by 1.2 to account for the missing peaks at 25–28 eV. The experimental ratio is estimated to be 8 ± 2.

The agreement between experimental and theoretical areas places some limitations on the possibilities that base-line or loss corrections to the Si $L_{23}VV$ will account for some of the experimental intensity in the 50-eV peak. If one changed either base-line or loss corrections in such a way as to lower the 50-eV peak area relative to the 78-eV peak, then the same correction would likely reduce the 40-eV $L_1L_{23}V$ peak area relative to the 78-eV peak. The result might be an unacceptable increase in the measured $L_{23}VV/L_1L_{23}V$ area ratio. Nevertheless the 50-eV peak is small and we cannot rule out the possibility that base-line and loss correction errors are

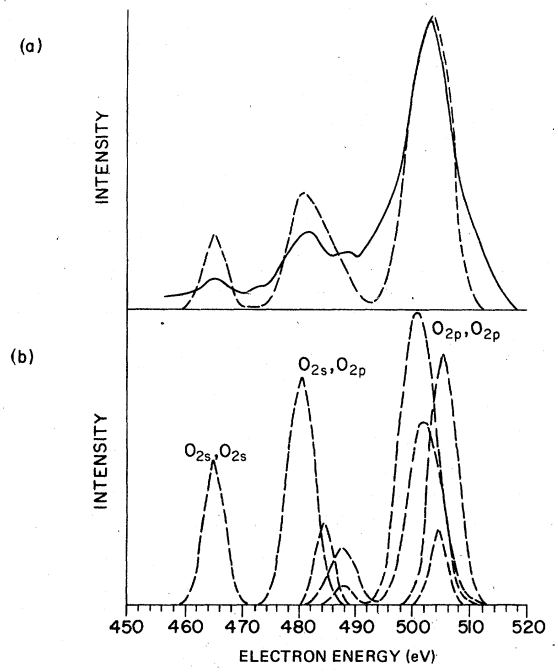

FIG. 6. (a) A comparison of the experimental (solid line) O KVV Auger line shape with those calculated from the $(SiO_2)_2$ populations (dashed line). The peak at 504 eV involves transitions with both valence electrons from the O_{2p} nonbonding and bonding groups; the peaks at 480 eV, one each from an O_{2p} and O_{2s} group; the peak at 465 eV, both from the O_{2s} group. (b) The major Auger transitions arising from the individual molecular orbitals which have local oxygen electron density. The origin of each peak may be identified from Table II.

significantly altering the experimental ratio of the 50- to 70-eV peaks.

The last transition is the O *KVV*; the comparison of theory and experiment are shown in Fig. 6. The theoretical energies were shifted down by less than 1 eV to bring the two line shapes into registry. Shirley's[58] calculation of the Ne gas-phase Auger energy was in error by 3 eV; he ascribed his error to the relaxation energy and we have assumed the same relaxation energy in this paper. Thus we must regard the close agreement here as somewhat fortuitous.

Shake-up and shake-off contributions to the oxygen Auger peaks[61,62] may account for much of the areas between the major peaks which are underestimated by the calculated line shape. However, the O *KVV* theoretical line shape overestimates the relative intensities in the $O_{2p}O_{2s}$, $O_{2s}O_{2s}$ peaks compared with the $O_{2p}O_{2p}$ peak (see Fig. 6). This cannot be accounted for by shake-up or shake-off. The same factors which might have contributed to the Si $L_{23}VV$ discrepancies can be examined as sources of the discrepancies here. The use of the atomic matrix elements to calculate the O *KVV* intensities must be even more suspect than it was for the Si Auger calculations. Whereas for Si each major observed peak involves principally p-p and s-p transitions, in the case of oxygen the three peaks at 503, 481, and 465 eV involve different atomic matrix elements, p-p, s-p, and s-s, respectively. The correct relationship between these three matrix elements is not even assured in the atomic case. For instance, for elements near oxygen experiment shows the s-p/p-p matrix-element ratio to be substantially smaller than that predicted by the theoretical matrix elements that we used in this paper.[53] If our assumed s-p/p-p ratio were decreased our present overestimation of the s-p Auger peak would improve.

The possibility of a different charge balance between the O_{2p} and O_{2s} orbitals accounting for the observed discrepancy in the O *KVV* line shapes can be examined. The only other electron spectroscopy to sample both the O_{2s} and O_{2p} electron densities is photoelectron spectroscopy. From the XPS measurements of DiStefano and Eastman[12] one can measure the areas under the O_{2p} and O_{2s} orbital groups (estimating an appropriate background as base line); the ratio of these areas is $A(O_{2p})/A(O_{2s}) \cong 0.6$. Unfortunately, the XPS measurement is not sensitive to the local oxygen electron density and also samples the electrons localized on the Si. From the XPS cross sections of Scofield[64] and the populations of Table III(b) we estimate that the O_{2s} area is essentially pure oxygen (~2% correction for Si electrons) and the O_{2p} area needs to be multiplied by about 0.8 to correct for Si electrons. The ratio of cross sections for the Al K_α excitation of the oxygen valence electrons is given by Scofield[64] as $\sigma_{2s}/\sigma_{2p} = 6.4$. The XPS measurement of the electron population ratio is then $O_{2p}/O_{2s} = 0.6 \times (6.4) \times 0.8 \cong 3$. The equivalent ratio calculated from the populations of Table III(b) is 2.8; to get the Auger line shapes to agree, this ratio would have to increase to 3.5. Given the uncertainties in the XPS ratio either 2.8 or 3.5 could be taken as agreeing with the XPS measured ratio.

Returning to an earlier point, recall that when the populations in Table II were established, we ignored the highest-energy peak in the Si L_{23} x-ray emission spectrum (see Fig. 3). The origin of this peak is the subject of considerable debate.[56] Since the equivalent peak appears in the L_{23} spectra of S in SO_4^{2-} and P in PO_4^{3-}, one cannot write it off simply as contamination. It may arise from defects due to beam damage, but no one has spoken of observing a beam-exposure dependence of its intensity. According to the L_{23} selection rules, it may be s- or d-localized Si electrons. If it were to be Si s-like electrons, then the large intensity observed in the L_{23} spectra should be replicated in the Si $L_1L_{23}V$ Auger spectra about 2 eV above the $4t_2$ orbital. But no such peak is observed. If Si $3d$ electrons are the source, then we might expect the electron repulsion term $F(X, Y)$ of the L_1L_{23} $3d$ Auger transition to be smaller, and the Auger transition energy thereby larger than for $3s$ electrons. Further the intensity matrix element may be smaller. This raises the possibility that a $L_1L_{23}V$ transition involving $3d$ electrons may be hidden in the energy region between the identified $L_1L_{23}V$ and $L_{23}VV$ transitions. The presence of $3d$ electrons may also account for our underestimation of the high-energy side of the $L_{23}VV$ transition.

Finally, as a last point of discussion, we consider the hole-hole interaction effects. An energy shift of less than 2 eV (in all cases the theory must be shifted down) is required to bring the theoretical and measured major peak of each line shape into registry. Excellent agreement is found between the calculated and experimental energies of all peaks in the three line shapes after registry of the major peaks. Unfortunately the magnitude of the hole-hole repulsion and static relaxation effects $U = R(x, y) - F(x, y)$ for the various transitions within each line shape is fairly constant; therefore the agreement between theory and experiment of the relative energy of the peaks in the line shapes is not a critical test of the MO model. For the Si line shapes, the

average value of $U = R - F$ obtained from the cluster MO model is small, +1.5 for Si $L_1L_{23}V$, −2.3 for Si $L_{23}VV$. The Si 3*s* and 3*p* orbital splitting is ≈14 eV providing an estimate of V; Γ is ≈ 2 eV (Table I). For a single Si atom $U \approx 7$ eV.[57] Thus, hole-hole correlation should cause heavy mixing of the states within the band, but little mixing of the cluster MO states. Note how quickly the effective U decreases as the holes delocalize from the Si atom to the SiO_4^{4-} cluster. For the O *KVV* line shape, U is ≈ 14 eV as calculated in the MO cluster model (Table II). The O 2*s* and 3*p* orbitals split by about 2–3 eV, Γ is again about 2 eV (Table I). For a single O atom $U \approx 14$ eV.[57] In this instance $U > V \approx \Gamma$ and the final two-hole DOS should be atomiclike. Note that the effective U calculated in the MO model is equal to that of the single atom. This is true because the major Auger contributions in the O *KVV* line shape come from those MO's almost completely localized on the atom (this was not true on the Si). That the O *KVV* line shape in SiO_2 is essentially atomiclike can be substantiated by comparing it with the O *KVV* line shape in the more ionic MgO.[65] They are essentially identical. The one-electron cluster MO model has properly accounted for the hole-hole interactions for both the Si and O Auger line shapes, even though the degree of delocalization is quite different in the two cases.

In summary we have calculated the Si $L_1L_{23}V$, Si $L_{23}VV$, and O *KVV* Auger line shapes for SiO_2 utilizing the cluster MO model and compared them to experimentally derived line shapes. In all three cases the energies of the major features are in agreement to within the uncertainties in the calculations and measurements. The most likely sources of the major discrepancies in intensity are considered to be the assumed matrix elements and electron populations, and the neglect of Auger satellite contributions.

ACKNOWLEDGMENT

Research by M. G. Lagally, G. Moore, and J. Houston was supported by Department of Energy.

[1]M. H. Reilly, J. Phys. Chem. Solids 31, 1041 (1970).
[2]D. S. Urch, J. Phys. C 3, 1275 (1970).
[3]A. J. Bennett and L. M. Roth, J. Phys. Chem. Solids 32, 1251 (1971).
[4]T. L. Gilbert, W. J. Stevens, H. Schrenk, M. Yoshimine, and P. S. Bagus, Phys. Rev. B 8, 5877–5998 (1973).
[5]K. L. Yip and W. B. Fowler, Phys. Rev. B 10, 1400–1408 (1974).
[6]G. A. D. Collins, D. W. J. Cruickshank, and A. Breeze, J. Chem. Soc. Faraday Trans. II 68, 1189–1195 (1972).
[7]J. A. Tossell, J. Phys. Chem. Solids 34, 307–319 (1973).
[8]J. A. Tossell, D. J. Vaughan, and K. H. Johnson, Chem. Phys. Lett. 20, 329–334 (1973).
[9]S. T. Pantelides and W. A. Harrison, Phys. Rev. B 13, 2667–2691 (1976).
[10]P. M. Schneider and W. B. Fowler, Phys. Rev. Lett. 36, 425 (1976).
[11]J. R. Chelikowsky and M. Schluter, Phys. Rev. B 15, 4020–4029 (1977).
[12]T. H. DeStefano and D. E. Eastman, Phys. Rev. Lett. 27, 1560 (1971).
[13]H. Ibach and J. E. Rowe, Phys. Rev. B 10, 710 (1974).
[14]J. E. Rowe, Appl. Phys. Lett. 25, 576 (1974).
[15]B. Fischer, R. A. Pollak, T. H. DeStefano, and W. D. Grobman, Phys. Rev. B 15, 3193–3199 (1977).
[16]G. Klein and H. U. Chun, Phys. Status Solidi B 49, 167 (1972).
[17]D. W. Fischer, J. Chem. Phys. 42, 3814 (1965).
[18]G. Wiech, in *Soft X-Ray Band Spectra*, edited by D. J. Fabian (Academic, New York, 1968), p. 59.
[19]O. A. Ershov, D. A. Goyonov, and A. P. Lukirskii, Sov. Phys. Solid State 7, 1903 (1966).
[20]M. K. Bernett, J. S. Murday, and N. H. Turner, J. Electron Spectrosc. Relat. Phenom. 12, 375–393 (1977).
[21]J. S. Johannessen, W. E. Spicer, and Y. E. Strausser, J. Vac. Sci. Technol. 13, 849–855 (1976).
[22]L. Fiermans, R. Hoogewijs, and J. Vennik, Surf. Sci. 47, 1–4 (1975).
[23]J. S. Soloman and W. L. Baun, Surf. Sci. 51, 228–236 (1975).
[24]S. Ferrer, A. M. Baro, and J. M. Rojo, Surf. Sci. 64, 668–680 (1977).
[25]J. H. Fox. J. D. Nuttall, and T. E. Gallon, Surf. Sci. 63, 390–402 (1977).
[26]S. P. Kowalczyk, L. Ley, F. R. McFeely, R. A. Pollak, and D. A. Shirley, Phys. Rev. B 9, 381–391 (1974).
[27]H. H. Madden and J. E. Houston, J. Vac. Sci. Technol. 14, 412–415 (1977); Solid State Commun. 21, 1081 (1977).
[28]J. M. Burkstrand and G. G. Tibbetts, Phys. Rev. B 15, 5481–5483 (1977).
[29]P. J. Feibelman, E. J. McGuire, and K. C. Pandey, Phys. Rev. B 15, 2202 (1977); P. J. Feibelman and E. J. McGuire, *ibid.* 17, 690 (1978).
[30]J. F. McGilp and P. Weightman, J. Phys. C 11, 643–650 (1978); 9, 3541–3556 (1976).
[31]D. R. Jennison, Phys. Rev. Lett. 40, 807–809 (1978); Phys. Rev. B 18, 6865–6871 (1978).
[32]D. R. Jennison, H. H. Madden, and D. M. Zehner, Phys. Rev. Lett. (to be published).
[33]H. H. Madden, D. M. Zehner, and J. R. Noonan, Phys. Rev. 17, 3074–3088 (1978).
[34]D. R. Jennison, Phys. Rev. B 18, 6996–6998 (1978).
[35]E. Antonides, E. C. Janse, and G. A. Sawatzky, Phys. Rev. B 15, 1669–1679 (1977).
[36]W. E. Moddeman, T. A. Carlson, M. O. Krause, B. P. Pullen, W. E. Bull, and G. K. Schweitzer, J. Chem. Phys. 55, 2317 (1971).
[37]R. W. Shaw, J. S. Jen, and T. D. Thomas, J. Electron Spectrosc. Relat. Phenom. 11, 91–100 (1977).

[38]K. Siegbahn, C. Nordling, G. Johansson, J. Hedman, P. F. Hedei, K. Hamrin, U. Gelius, T. Bergmark, L. O. Werme, R. Manne, and Y. Baer, *ESCA Applied to Free Molecules* (North-Holland, Amsterdam, 1969).
[39]D. R. Jennison, Chem. Phys. Lett. (to be published).
[40]D. E. Ramaker and J. S. Murday (unpublished).
[41]J. E. Houston, G. Moore, and M. G. Lagally, Solid State Commun. 21, 879–882 (1977).
[42]J. E. Houston, J. Vac. Sci. Technol. 12, 255 (1975).
[43]M. Cini, Solid State Commun. 20, 605–607 (1976); Phys. Rev. B 17, 2788 (1978).
[44]G. A. Sawatzky, Phys. Rev. Lett. 39, 504–507 (1977).
[45]Samples were grown by H. Guckel, I. C. Laboratory, University of Wisconsin, Madison.
[46]R. Ludeke and E. Koma, Phys. Rev. Lett. 35, 107 (1975).
[47]D. E. Ramaker, J. S. Murday, and N. H. Turner, J. Electron Spectrosc. Relat. Phenom. (to be published).
[48]E. N. Sickafus, Rev. Sci. Instrum. 42, 533 (1971).
[49]W. M. Mularie and W. T. Peria, Surf. Sci. 26, 125 (1971).
[50]G. D. Davis and M. G. Lagally, J. Vac. Sci. Technol. 15, 1311–1316 (1978).
[51]D. Welkie and M. G. Lagally (unpublished).
[52]P. H. Van Cittert, Z. Phys. 69, 304 (1931).
[53]E. J. McGuire, Phys. Rev. 185, 1–6 (1969); Phys. Rev. A 3, 587–594 (1971).
[54]D. L. Walters and C. P. Bhalla, Phys. Rev. A 4, 2164–2170 (1971).
[55]B. Carriere and B. Lang, Surf. Sci. 64, 209–223 (1977).
[56]D. L. Griscom, J. Non-Cryst. Solids 24, 155–234 (1977).
[57]J. B. Mann, Los Alamos Scientific Laboratory Report No. LASL-3690, 1967 (unpublished).
[58]D. A. Shirley, Phys. Rev. A 7, 1520–1528 (1973).
[59]F. A. Gianturco and C. A. Coulson, Mol. Phys. 14, 223–232 (1968).
[60]K. Taniguchi and B. L. Henke, J. Chem. Phys. 64, 3021–3035 (1976).
[61]M. O. Krause, T. A. Carlson, and W. E. Moddeman, J. Phys. (Paris), Colloq. C4 32, 139–144 (1971); M. O. Krause, F. A. Stevie, L. J. Lewis, T. A. Carlson, and W. E. Moddeman, Phys. Lett. A 31, 81–82 (1970).
[62]W. Mehlhorn, Z. Phys. 208, 1–27 (1968); W. Melhorn and D. Stalhem, *ibid.* 217, 294–303 (1968).
[63]E. J. McGuire, Phys. Rev. A 16, 73–79 (1977).
[64]J. H. Scofield, J. Electron Spectrosc. Relat. Phenom. 8, 129–137 (1976).
[65]P. J. Bassett, T. E. Gallon, M. Prutton, and J. A. D. Matthew, Surf. Sci. 33, 213–218 (1972).